ARTICLES

Prion recognition elements govern nucleation, strain specificity and species barriers

Peter M. Tessier[1] & Susan Lindquist[2]

Prions are proteins that can switch to self-perpetuating, infectious conformations. The abilities of prions to replicate, form structurally distinct strains, and establish and overcome transmission barriers between species are poorly understood. We exploit surface-bound peptides to overcome complexities of investigating such problems in solution. For the yeast prion Sup35, we find that the switch to the prion state is controlled with exquisite specificity by small elements of primary sequence. Strikingly, these same sequence elements govern the formation of distinct self-perpetuating conformations (prion strains) and determine species-specific seeding activities. A Sup35 chimaera that traverses the transmission barrier between two yeast species possesses the critical sequence elements from both. Using this chimaera, we show that the influence of environment and mutations on the formation of species-specific strains is driven by selective recognition of either sequence element. Thus, critical aspects of prion conversion are enciphered by subtle differences between small, highly specific recognition elements.

The ability of proteins to form β-sheet-rich amyloids is associated not only with disease[1], but also with diverse normal biological functions, including cell adhesion[2], skin pigmentation[3], adaptation to environmental stresses[4–6] and perhaps even long-term neuronal memory[7]. Prions are an unusual class of amyloid-forming proteins, whose conformations are self-templating (self-seeding) and thereby infectious. The conformationally converted prion state can be transmitted from cell to cell within or, in some cases, between organisms. Prions, too, can be either deadly or beneficial[4–6,8].

The first identified prion protein was PrP, whose conversion to the prion conformer (PrP^{Sc}) is associated with several fatal neurodegenerative diseases[8]. More recently, several prions in yeast and other fungi have been identified that are unrelated to PrP or one another[9–12]; some of these may have beneficial effects[4–6]. The most well-studied is Sup35 (refs 13, 14), a translation-termination factor whose conversion to the prion state reduces its activity. This increases the read-through of stop codons, revealing hidden genetic variation and creating complex new phenotypes in a single step[4–6].

Sup35 prions exhibit two of the most baffling aspects of prion biology that were initially identified for mammalian PrP. First, both Sup35 and PrP can adopt not just one prion conformation, but a suite of related yet structurally distinct conformations (known as strains or variants)[15–21]. Each conformation self-perpetuates and confers a distinct biological phenotype. Second, the transmission of the prion state between proteins of different species is limited by a species barrier that can occasionally be traversed[22–33]. In both yeast and mammals the ability to establish and overcome species barriers is, in some unknown way, related to the ability of prions to form distinct strains[8,13,24,31,33–37].

The carboxy-terminal domain of Sup35 encodes the translation-termination function[13,14]. Whether Sup35 exists in either a prion or a non-prion state is controlled by the interplay of two other domains[13,14]. The middle region (M) has a strong solubilizing activity and is very rich in charged residues. The amino (N) terminus is extremely amyloidogenic and of unusually low sequence complexity, composed primarily of glutamine, asparagine, glycine and tyrosine residues (Supplementary Fig. 1).

In its non-prion state NM is compact, but molten, rapidly fluctuating through diverse conformations[38]. The structure of NM in its prion state is heavily debated. Several lines of evidence suggest that two discrete regions of the N domain are in self-contact within NM fibres[39]; the region between them is sequestered from intermolecular contacts, whereas elements proximal and distal to the contacts are not part of the amyloid core. Cross-linking NM molecules at one of the intermolecular contacts, but not elsewhere, accelerates nucleation[39]. However, other lines of evidence suggest that most residues of the N domain are in intermolecular contact, stacking in-register on themselves[40–43]. Genetic evidence is also in conflict. Single substitution mutations in certain regions of the N terminus can have profound effects on many aspects of prion biology: they can inhibit replication[44,45], bias prion conversion towards the production of distinct strains[36,45], and increase or decrease the ability of prions to cross species barriers[36]. These studies would indicate that precise features of amino acid sequence have critical roles in Sup35 prion biology. Remarkably, however, scrambling the sequence of N does not prevent prion formation[42,43]. This argues that NM prion formation is mainly dependent on the amino acid composition and largely independent of primary sequence[42,43].

To shed light on these paradoxes, and to bring new technology to bear on the baffling relationship between prion strains and species barriers, we have employed surface-bound arrays of prion peptides. We find that small elements of the *Saccharomyces cerevisiae* Sup35 sequence govern prion recognition with extraordinary specificity. We exploited the properties of such sequences to identify critical prion recognition elements *de novo* in a distantly related yeast species. Remarkably, the recognition elements identified using peptide arrays

[1]Whitehead Institute for Biomedical Research, 9 Cambridge Center, Cambridge, Massachusetts 02142, USA. [2]Howard Hughes Medical Institute, Whitehead Institute for Biomedical Research, 9 Cambridge Center, Cambridge, Massachusetts 02142, USA.

govern nucleation, the formation of distinct prion strains and the capacity of prions to cross species-specific transmission barriers.

Identification of prion recognition elements

We sought to determine how natively unfolded non-prion conformers achieve self-recognition. Is it encoded by specific sequence elements? Or is it a distributed property of the N domain's unusual low-complexity sequence? To investigate this question we sought to interrogate the affinity of full-length proteins for diverse short elements of the NM sequence. However, short peptides from aggregation-prone proteins are often poorly soluble, precluding assessment of such interactions in solution.

To overcome this problem, we arrayed a library of overlapping denatured 20-mer peptides derived from the sequence of the prion domain of *S. cerevisiae* Sup35 (ScNM) on glass slides. An extensive library of 136 overlapping peptides from ScNM was synthesized. Each peptide carried 20 residues of prion sequence at its C terminus, preceded by a 14-carbon hydrophilic spacer and an N-terminal, double lysine tag for covalent immobilization. The peptides, which should occupy ~2–3 nm in a random coil conformation under these conditions, were printed with an average spacing of ~10–12 nm to restrict self-interactions. Each peptide sequence was shifted from that of the preceding peptide by one to six residues. In the final version of the arrays smaller intervals were employed to provide higher resolution in critical regions that were identified in preliminary experiments. (The density of coverage is indicated by the spacing of the bars in the figures, with the *x*-axis referencing the centre residue of the peptide.) The ability of the immobilized peptides to interact with soluble, full-length NM was examined by incubating fluorescently labelled protein with the peptide arrays. The label was introduced via a cysteine substitution mutation (alanine to cysteine at residue 230, A230C) located in a region that lies far from the residues involved in prion formation[39,44].

Incubating full-length ScNM with the peptide arrays for two hours led to a strong accumulation of label over only a very small set of peptides: those encompassing amino acids 9–28, 10–29, 11–30, 12–31 and 20–39 (Fig. 1a, b and Supplementary Table 2). These interactions were highly reproducible (Fig. 1a). Strikingly, these sequences lie within the region previously found by mutational analysis[44] and crosslinking[39] to strongly influence ScNM prion assembly. They also overlap with one of two regions previously identified as being in self-contact within mature fibres[39].

To determine if other peptide regions could interact with ScNM, albeit with lower efficiency, we took advantage of the fact that the spontaneous assembly of the full-length protein, even at fivefold higher concentrations, is very slow in quiescent reactions[46]. At this concentration and with a higher fraction of the protein carrying the fluorescent probe (75% versus 5% of protein), label could be detected at a second set of peptides, spanning residues ~90–120 after one to two days (Fig. 1c, Supplementary Table 2 and data not shown). This region corresponded to the second previously identified site of intermolecular contact within mature ScNM fibres (~85–105)[39]. The reactivity of the surface-bound peptides indicates that these regions are not only sites of intermolecular contact in mature fibres[39], but also represent highly specific self-recognition elements within soluble molten, non-prion conformers.

Recognition elements nucleate NM amyloids

What is the nature of the protein bound to the peptide arrays? The fluorescence detected at specific peptide spots after two hours (Fig. 1d) continued to increase after even a full day of incubation (Fig. 1e). In a further attempt to saturate peptide reactivity on the arrays, the slides were pre-incubated with unlabelled ScNM for five days. However, when subsequently incubated with labelled protein, these spots continued to accumulate label as above (Fig. 1f).

These results indicated that the growing signals at specific spots might not simply be due to slow recognition of rare soluble conformers. Rather, they might represent sites of prion assembly. Indeed, the fluorescent signal was resistant to extensive washing with 2% SDS, a characteristic of NM amyloids[46]. Further, when the material accumulating at these specific spots was scraped from the slide and imaged by transmission electron microscopy, abundant fibres with the characteristic diameter of NM prion fibres[47] were observed (Fig. 1g).

The concentration of peptides in the arrayed spots is ~300-fold greater than the protein in bulk solution. Thus, soluble proteins might achieve critical nucleating contacts with peptides on the arrays more rapidly than with other full-length proteins in solution. However, the striking correspondence between the peptides at which fibres accumulated and the amino-acid segments that form intermolecular contacts in mature ScNM amyloids[39] suggests an alternative explanation: the peptides might capture ScNM amyloids that assemble in solution during the incubation. To test this, labelled ScNM fibres were sonicated into small fragments and incubated with the arrays. The fluorescence that accumulated at peptide spots was broadly distributed and similar to background (data not shown). We conclude that the fibres associated with specific peptide spots assembled there *in situ* from soluble NM. It was not possible to determine whether the interacting soluble species is monomeric or oligomeric. Regardless, our data establish that with an extraordinary

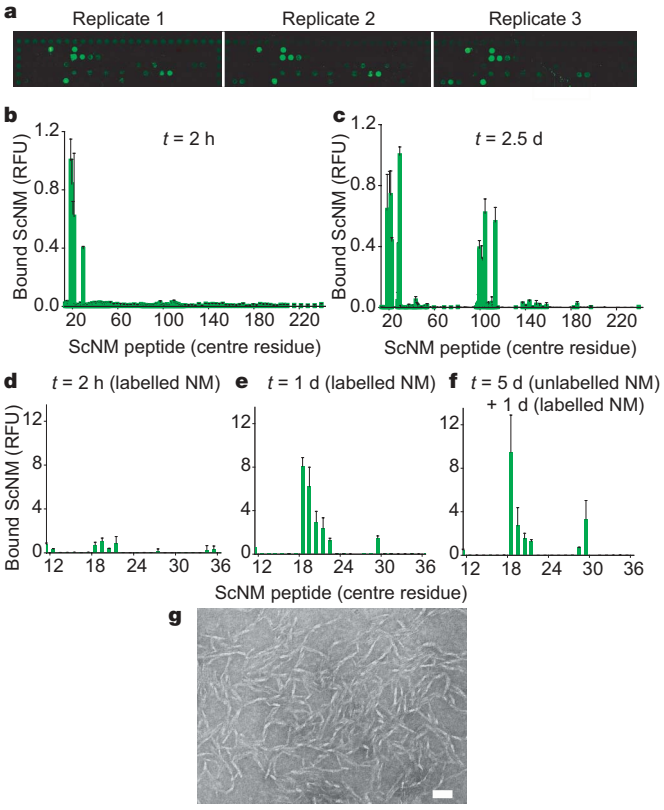

Figure 1 | Identification of recognition sequences within ScNM using peptide arrays. **a**, Image of a triplicate array of sequential overlapping 20-mer ScNM peptides after incubation with labelled full-length ScNM. **b–c**, Quantification of the fluorescence of labelled full-length ScNM bound to a similar peptide array after two hours (**b**; 1 μM, 5% Alexa Fluor 555) and two and a half days (**c**; 5 μM, 75% Alexa Fluor 555). The relative fluorescence intensity (RFU) for each 20-mer peptide is displayed at its central residue on the *x* axis. **d–f**, Quantification of the fluorescence of labelled full-length ScNM (1 μM, 5% Alexa Fluor 555) bound to ScNM peptides after two hours (**d**), one day (**e**) and one day after preincubation with unlabelled full-length ScNM (1 μM) for five days (**f**). **g**, Transmission electron micrograph of full-length ScNM fibres that assembled on a peptide array after two and a half days. The scale bar is 50 nm. For **b** and **c**, the fluorescence at each time point was normalized to the maximum fluorescence at that time point (set at 1.0). For **d–f**, fluorescence was normalized to the maximum value in **d** (set at 1.0). All fluorescence values are reported as median + s.d.

degree of specificity small elements of the Sup35 prion sequence are able to recognize molten conformers of full-length NM and convert them via this recognition to a self-templating state.

Candida albicans NM behaves in a similar manner

Next, we asked if another prion protein might have specific, highly localized recognition elements and if our method could be used to identify them. We employed the homologous prion domain of Sup35 from *C. albicans*, a species separated from *S. cerevisiae* by >800 million years[48]. The sequence of *C. albicans* NM (CaNM) shares no significant tracts of alignable sequence with *S. cerevisiae* NM[23], but is of similar low complexity and amino acid composition (Supplementary Fig. 1). CaNM was fluorescently labelled and incubated with a library of 128 overlapping CaNM peptides. After two hours, CaNM reacted in a highly-specific manner with a small cluster of peptides: amino acids 59–78, 60–79, 61–80, 62–81, 63–82, 66–85 and 67–86 (Fig. 2a and Supplementary Table 3). After longer incubations (one to two days) at fivefold higher CaNM concentrations, and with a higher fraction of the protein carrying the fluorescent probe (75% versus 5% of protein), label accumulated at a second set of peptides, spanning residues ~110–130 (inset of Fig. 2a, Supplementary Table 3 and data not shown). As with ScNM, the signals obtained with CaNM were not saturable and continued to increase over several days of incubation (data not shown). Further, the signals were resistant to extensive washing with 2% SDS. Remarkably, for two distantly related yeast species, short peptides from two distinct regions of the prion domain display a similar pattern of recognition by the full-length soluble proteins and a similar capacity to convert them, via this recognition, to a self-templating state.

Reconstitution of the species barrier on arrays

Prion fibres of *S. cerevisiae* and *C. albicans* Sup35 can seed the polymerization of their own proteins, but a species barrier prevents efficient cross-seeding[22,23,34,36]. The striking specificity by which specific peptides interact with and nucleate assembly of full-length ScNM and CaNM prompted us to ask if the species barrier could be explained by the recognition elements uncovered by the peptide arrays. Indeed, when labelled, full-length ScNM was incubated with a peptide array displaying 128 CaNM peptides for two hours, no association was detected above background (Fig. 2b). The interaction of ScNM with peptides in its own recognition element (encompassing residues 9–39) was at least 30 fold greater than its interaction with any of the CaNM peptides. Conversely, incubating labelled full-length CaNM with an array displaying 136 ScNM peptides produced only background levels of fluorescence (Fig. 2c). The interaction of CaNM with its own peptides (encompassing residues 59–86) was 28-fold greater than for any of the ScNM peptides. This high degree of specificity was maintained even after two days (data not shown).

To test the strength of the species barrier observed on the peptide arrays more stringently, we mixed proteins of both species, each labelled with a different colour dye (ScNM, green; CaNM, red), and incubated them with arrays containing both peptides. The NM proteins of each species interacted only with a small subset of peptides from their own sequences (Fig. 2d).

Next, we employed a promiscuous *S. cerevisiae*/*C. albicans* NM chimaera that has been shown previously to traverse the species barrier between *S. cerevisiae* and *C. albicans*[22,36]. This chimaeric protein contains segments from both ScNM and CaNM (residues: *S. cerevisiae*, 1–40 and 124–253; *C. albicans*, 49–141; Supplementary Fig. S1)[22,36]. Incubating the full-length NM chimaera with an array displaying libraries of both ScNM and CaNM peptides revealed that it was able to interact with the prion recognition elements from both species in a highly specific manner (Fig. 2e).

Formation of species-specific prion strains

These results suggest that (1) the species barrier between ScNM and CaNM can be defined in terms of the differential affinities of soluble protein for specific short sequence elements that have the capacity to initiate a self-templating state, and (2) crossing this barrier is based on the ability of soluble protein to interact promiscuously with sequence elements from both species. To test these hypotheses more rigorously, we exploited the ability of the Sc/Ca NM chimaera to assemble into distinct strains that have species-specific seeding activities[22,34,36]. Protein fibres assembled from the chimaeric protein at 15 °C seed amyloid formation of ScNM but not CaNM[36]. Fibres assembled at 37°C have the opposite specificity[36]. For ease of manipulation we confirmed that the species-specific strain properties obtained at 15 °C were also obtained at 4 °C at the protein concentrations employed for our arrays (data not shown).

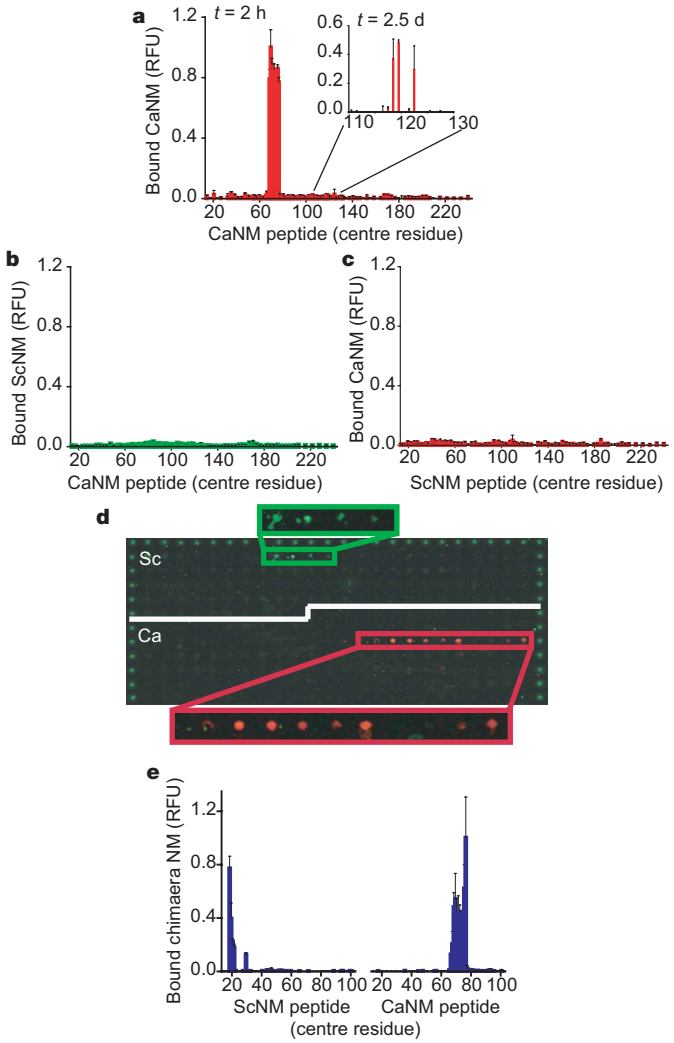

Figure 2 | Analysis of CaNM recognition sequences and the species barrier between *S. cerevisiae*/*C. albicans* NM. **a**, Quantification of the fluorescence of labelled full-length CaNM bound to overlapping 20-mer CaNM peptides after two hours (1 μM, 5% Alexa Fluor 647) and two and a half days (inset, 5 μM, 75% Alexa Fluor 647). The fluorescence at each time point was normalized to the maximum fluorescence at that time point (set at 1.0). **b**, Quantification of the fluorescence of labelled full-length ScNM (1 μM, 5% Alexa Fluor 555) bound to overlapping 20-mer CaNM peptides after two hours. **c**, Quantification of the fluorescence of labelled full-length CaNM (1 μM, 5% Alexa Fluor 647) bound to overlapping 20-mer ScNM peptides after two hours. **d**, Image of a single peptide array that was simultaneously incubated with labelled full-length ScNM (green, Alexa Fluor 555) and CaNM (red, Alexa Fluor 647) for two hours (1 μM final concentration of each protein, 5% label). **e**, Quantification of the fluorescence of labelled full-length Sc/Ca NM chimaera (1 μM NM, 5% Alexa Fluor 647) bound to both ScNM and CaNM peptides after two hours of incubation. All fluorescence values are reported as median + s.d.

As described above, when the chimaeric protein was incubated with the peptide arrays at 25 °C, it interacted with peptides from both species (Fig. 2e). However, at 37 °C it interacted selectively with CaNM peptides (Fig. 3a). At 4 °C it interacted selectively with ScNM peptides (Fig. 3b). Thus, the ability of the chimaeric protein to assemble into distinct species-specific strains at different temperatures is enciphered by the same small sequence elements that nucleate amyloid assembly.

Next, we tested the hypothesis that the effects of mutations on the formation of species-specific strains could be explained by these same prion recognition elements. As previously reported, changing serine residue 17 to arginine (S17R) in the Sc/Ca chimaera favours assembly of a prion strain that selectively seeds CaNM[36]. Conversely, changing four glycines at positions 70, 71, 80 and 81 to alanines (4G/A) favours assembly of a strain that selectively seeds ScNM[36]. When the S17R chimaera was incubated with the arrays at 25 °C, binding to all ScNM peptides was reduced to background (Fig. 3c). Importantly, binding to CaNM peptides was unaffected (Fig. 3c). Similarly, when the 4G/A chimaera was incubated with the arrays, binding to all but one of the CaNM peptides was greatly reduced but binding to ScNM peptides was similar to the original chimaera (Fig. 3d).

Mechanism of prion recognition

How do the mutations in the Sc/Ca chimaera alter prion recognition and strain formation? They might bias the conformations sampled by the molten full-length proteins such that particular recognition elements are masked. Alternatively, they might directly interfere with interactions between the full-length proteins and their cognate recognition elements. To investigate this question, the ability of the original chimaeric protein to interact with arrays containing mutant peptides was tested. Labelled chimaeric protein bound robustly to the wild-type ScNM and CaNM peptides (dark blue bars, Fig. 4a and b). However, it exhibited no interaction above background with any ScNM peptides containing the S17R mutation (yellow bars, Fig. 4a) or any CaNM peptides containing the 4G/A mutations (pink bars, Fig. 4b). Because the original chimaera reacted with wild-type peptides on the same array, it must have displayed its own recognition element. Its inability to interact with the mutant peptides, therefore, indicates that the mutations directly disrupt the recognition function of the sequence elements rather than solely altering the conformations of the soluble protein. Thus, these mutations, which bias prions toward the formation of distinct strains and alter cross-species prion transmission, do so by directly interfering with recognition of the prion specificity elements.

Discussion

Using arrays of surface-bound peptides, we find that small elements of prion sequence govern self-recognition with exquisite specificity. These recognition elements are alone sufficient to drive the conversion of full-length NM in the non-prion conformation—molten,

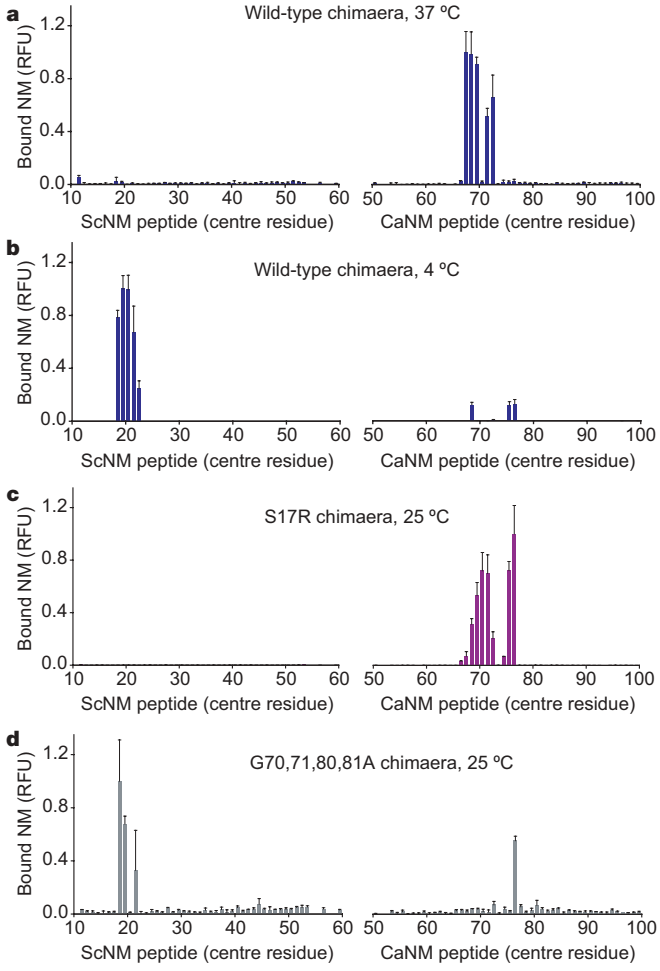

Figure 3 | Analysis of the conformational preference of the *S. cerevisiae*/*C. albicans* NM chimaera. **a**–**d**, Quantification of the relative binding of various labelled full-length NM chimaeric proteins to overlapping 20-mer ScNM and CaNM peptides: **a**, Sc/Ca chimaera at 37 °C; **b**, Sc/Ca chimaera at 4 °C; **c**, S17R Sc/Ca chimaera at 25 °C; and **d**, G70, 71, 80, 81A Sc/Ca chimaera at 25 °C. The peptide arrays were incubated with each prion domain (1 μM NM, 5% Alexa Fluor 647) for two hours. All fluorescence values are reported as median + s.d.

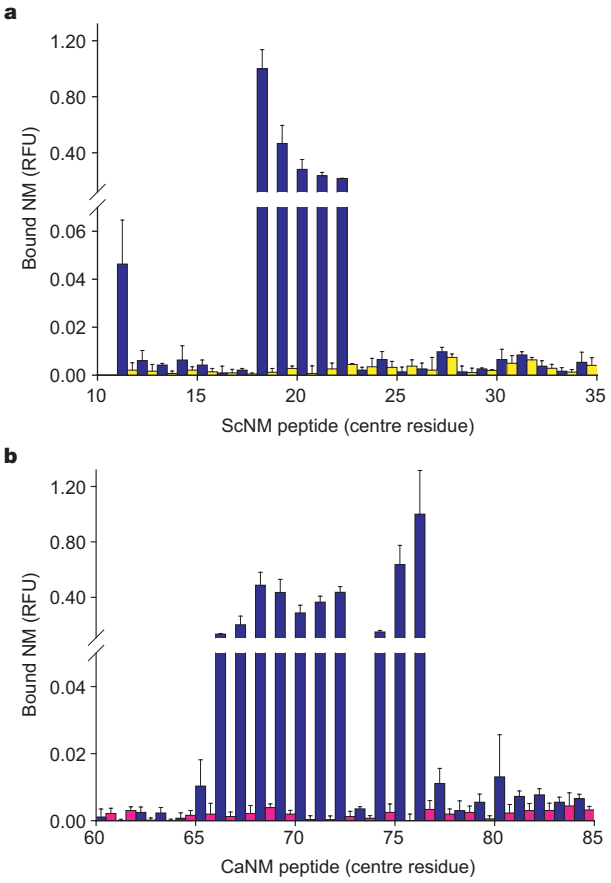

Figure 4 | Analysis of the mutational disruption of the ScNM and CaNM recognition elements. **a**, Quantification of the relative affinity of the full-length Sc/Ca NM chimaera for wild-type ScNM peptides (dark blue bars) and ScNM peptides containing the S17R mutation (yellow bars). **b**, Quantification of the relative affinity of the full-length Sc/Ca NM chimaera for wild-type CaNM peptides (dark blue bars) and CaNM peptides containing the G70, 71, 80, 81A mutations (pink bars). The peptide arrays were incubated with the NM chimaera (1 μM NM, 5% Alexa Fluor 647) for two hours. All fluorescence values are reported as median + s.d.

rapidly fluctuating, natively unfolded conformers—into self-templating amyloid conformations. Moreover, it is these same sequence elements that govern the formation of distinct prion strains and determine transmission barriers between species.

The highly localized and species-specific nature of the interactions detected with peptide arrays was unexpected for several reasons. For example, when the sequence of the *S. cerevisiae* Sup35 prion domain is scrambled, the protein still forms prions[42,43]. This had suggested that prion formation was a distributed property, owing to the unusual amino acid composition of the N domain, rather than a localized property of specific sequences within it. Indeed, scrambling of the prion domain sequence has occurred in nature for different yeast species. Although the *S. cerevisiae* and *C. albicans* N domains are both of low complexity (half of their residues are glutamines or asparagines and most others are tyrosines or glycines; Supplementary Fig. 1), their amino acid sequences cannot be aligned[23]. Yet CaNM forms prions with a similar efficiency as ScNM[22,23]. This, too, might suggest that prion formation is a distributed property governed primarily by amino acid composition.

However, full-length ScNM and CaNM interact with only a small number of peptides derived from their own sequences and do so in a highly localized and specific manner. But how can our data be reconciled with the ability of scrambled sequences to produce bona fide heritable prion elements? One explanation is that the scrambled NM sequences may form prions at very low efficiency; they were expressed at very high levels and their rates of prion conversion relative to the wild-type were not reported[42]. Alternatively, it may be that scrambling N domain sequences frequently results in the formation of new recognition elements. Given that the prion state produces many changes in phenotype (some detrimental and some beneficial)[4–6], the efficiency of prion conversion may have been conserved for ScNM and CaNM through selective pressures, despite sequence variation.

The peptides in the recognition elements we identified also have the unique capacity to drive molten non-prion conformers into a self-templating state. It has recently been reported that small amyloidogenic peptides from the N domain of ScNM (residues 7–12 and 7–13, which partially overlap with one of our recognition elements) can form microcrystals that yield high-resolution structures[49]. Our identification of critical nucleating peptides, therefore, holds promise for future high-resolution analysis of the bona fide templating structures of the yeast prion [PSI^+], and potentially the comparative analysis of such structures from organisms separated by 800 million years of evolution.

Remarkably, the non-prion conformers of both ScNM and CaNM interacted initially and most strongly with a small cluster of their own peptides towards the N-terminal side of the N domain (Figs 1b and 2a). Additionally, both proteins could interact with a second discrete cluster of their own peptides towards the C-terminal end of the N domain, but only after much longer incubations and at higher protein concentrations (Figs 1c and 2a, inset). This finding indicates that the nature of prion nucleation, conformational conversion and templating for Sup35 may have been conserved during evolution. If true, this would provide strong evidence for our previous hypothesis that the phenotypic variation created when Sup35 switches to the prion state is of considerable biological importance[4,5].

It is striking that the specific recognition sites identified on the arrays correspond to regions of intermolecular association identified in ScNM fibres by other methods[39]. Although our results cannot distinguish between proposed structural models for ScNM prion fibres[39–41], the data seem most consistent with one of them[39]: that two distinct regions in the N domain are in self-contact, with the intervening region sequestered from intermolecular contacts, and regions distal and proximal to the contacts being outside the amyloid core[39]. They are also consistent with cross-linking data suggesting that one of the two contact sites has a dominant role in nucleation[39].

Our data also suggest a new framework for conceptualizing the formation of species barriers and prion strains. Species barriers are known to depend, in part, on the primary sequence of prions[22–33]. We find that they are determined by highly localized elements of amino acid sequence. Moreover, these are the very same elements that control nucleation. Species barriers are also known to be influenced by prion strains[8,13,24,31,33–37], but the molecular connection has been elusive. For the promiscuous Sc/Ca NM chimaera the remarkable concordance between the way that specific mutations and environmental conditions determine the particular peptides that can nucleate soluble chimaeric protein on the arrays (Fig. 3) and the way they determine the species-specific propagation of different chimaeric strains[36] suggests the following relationship—within the same region of the same protein, small elements of primary sequence can initiate distinct intermolecular recognition events that drive the formation of different amyloid structures. These same sequence elements are the intermolecular contact sites that are then involved in templating those structures to soluble protein for propagation of the prion strain.

From a methodological perspective, it is empowering that peptide arrays, which are typically used to study the specificities of folded proteins, can also be used to identify sequences that drive structural transitions in natively unfolded proteins. This method has the potential to illuminate many difficult problems in human disease biology related to the conformational conversion of amyloidogenic proteins. Peptide arrays might also be employed in high-throughput drug screens for compounds that prevent protein assembly, promote it, or redirect it to alternative forms. Finally, the fact that highly ordered amyloid fibres can be specifically nucleated and assembled at patterned sites on solid surfaces, and that this assembly process can be tightly controlled by simple changes in environmental conditions (for example, temperature), may have important implications for fabricating materials and devices with complex, nanostructured features.

Perhaps the most important implication of our work is that the very nature of protein folding for Sup35 prions is profoundly different from that of proteins with globular domains. The latter is typically governed by a large number of intramolecular interactions that collectively and cooperatively drive folding of the entire domain. In contrast, we find that the folding of two distantly related yeast prion proteins into amyloid fibres of defined tertiary structure is controlled by intermolecular interactions between very small elements of primary sequence. Peptide arrays offer an opportunity to determine whether other amyloidogenic proteins fold by a similar mechanism.

METHODS SUMMARY

ScNM and CaNM contained a C-terminal 7×His-tag, as did the Sc/Ca NM chimaera constructs except for S17R, which contained a 6×His-tag. The NM cysteine mutants at or near the C terminus (*S. cerevisiae* A230C, *C. albicans* S227C and all chimaeras at the extreme C terminus) were labelled with maleimide-functionalized Alexa Fluor 555 or 647 (Invitrogen).

Each peptide contained a double alanine tag at its N terminus, a 20-residue segment derived from the Sup35 sequences, a hydrophilic linker (1-amino-4,7,10-trioxa-13-tridecanamine succinimic acid[50]) and a double lysine tag at its C terminus. The peptides were then printed onto hydrogel glass slides (Nexterion Slide H, Schott) functionalized with reactive *N*-hydroxysuccinimide (NHS) ester moieties. The NM proteins were denatured in 6 M guanidine hydrochloride at 100 °C, and then diluted 125-fold to a final concentration of 1–5 μM NM and a label-per-protein molar ratio of 5–75%. Each peptide array was incubated individually with 2–3 ml of diluted NM without mixing. The peptide arrays were then washed extensively with 2% SDS, water and methanol, and then spun dry. The arrays were then imaged using a Genepix 4000A scanner and the median fluorescence values of two or three replicates for the peptide spots were quantified using Genepix Pro 6.0 software (Molecular Devices).

Full Methods and any associated references are available in the online version of the paper at www.nature.com/nature.

Received 19 March; accepted 16 April 2007.
Published online 9 May 2007.

1. Selkoe, D. J. Folding proteins in fatal ways. *Nature* **426**, 900–904 (2003).

2. Chapman, M. R. *et al.* Role of *Escherichia coli* curli operons in directing amyloid fiber formation. *Science* **295,** 851–855 (2002).
3. Fowler, D. M. *et al.* Functional amyloid formation within mammalian tissue. *PLoS Biol.* **4,** 100–107 (2006).
4. True, H. L. & Lindquist, S. L. A yeast prion provides a mechanism for genetic variation and phenotypic diversity. *Nature* **407,** 477–483 (2000).
5. True, H. L., Berlin, I. & Lindquist, S. L. Epigenetic regulation of translation reveals hidden genetic variation to produce complex traits. *Nature* **431,** 184–187 (2004).
6. Eaglestone, S. S., Cox, B. S. & Tuite, M. F. Translation termination efficiency can be regulated in *Saccharomyces cerevisiae* by environmental stress through a prion-mediated mechanism. *EMBO J.* **18,** 1974–1981 (1999).
7. Si, K., Lindquist, S. & Kandel, E. R. A neuronal isoform of the Aplysia CPEB has prion-like properties. *Cell* **115,** 879–891 (2003).
8. Prusiner, S. B. Prions. *Proc. Natl Acad. Sci. USA* **95,** 13363–13383 (1998).
9. Wickner, R. B. & Masison, D. C. Evidence for two prions in yeast: [URE3] and [PSI]. *Curr. Top. Microbiol. Immunol.* **207,** 147–160 (1996).
10. Wickner, R. B. [Ure3] as an altered Ure2 protein: evidence for a prion analog in *Saccharomyces cerevisiae. Science* **264,** 566–569 (1994).
11. Sondheimer, N. & Lindquist, S. Rnq1: an epigenetic modifier of protein function in yeast. *Mol. Cell* **5,** 163–172 (2000).
12. Coustou, V., Deleu, C., Saupe, S. & Begueret, J. The protein product of the *het-s* heterokaryon incompatibility gene of the fungus *Podospora anserina* behaves as a prion analog. *Proc. Natl Acad. Sci. USA* **94,** 9773–9778 (1997).
13. Chien, P., Weissman, J. S. & DePace, A. H. Emerging principles of conformation-based prion inheritance. *Annu. Rev. Biochem.* **73,** 617–656 (2004).
14. Tuite, M. F. & Cox, B. S. Propagation of yeast prions. *Nature Rev. Mol. Cell Biol.* **4,** 878–890 (2003).
15. King, C. Y. & Diaz-Avalos, R. Protein-only transmission of three yeast prion strains. *Nature* **428,** 319–323 (2004).
16. Tanaka, M., Chien, P., Naber, N., Cooke, R. & Weissman, J. S. Conformational variations in an infectious protein determine prion strain differences. *Nature* **428,** 323–328 (2004).
17. Bruce, M. E., McConnell, I., Fraser, H. & Dickinson, A. G. The disease characteristics of different strains of scrapie in *Sinc* congenic mouse lines: implications for the nature of the agent and host control of pathogenesis. *J. Gen. Virol.* **72,** 595–603 (1991).
18. Caughey, B., Raymond, G. J. & Bessen, R. A. Strain-dependent differences in β-sheet conformations of abnormal prion protein. *J. Biol. Chem.* **273,** 32230–32235 (1998).
19. Kocisko, D. A. *et al.* Cell-free formation of protease-resistant prion protein. *Nature* **370,** 471–474 (1994).
20. Safar, J. *et al.* Eight prion strains have PrP(Sc) molecules with different conformations. *Nature Med.* **4,** 1157–1165 (1998).
21. Derkatch, I. L., Chernoff, Y. O., Kushnirov, V. V., Inge-Vechtomov, S. G. & Liebman, S. W. Genesis and variability of [PSI] prion factors in *Saccharomyces cerevisiae. Genetics* **144,** 1375–1386 (1996).
22. Chien, P. & Weissman, J. S. Conformational diversity in a yeast prion dictates its seeding specificity. *Nature* **410,** 223–227 (2001).
23. Santoso, A., Chien, P., Osherovich, L. Z. & Weissman, J. S. Molecular basis of a yeast prion species barrier. *Cell* **100,** 277–288 (2000).
24. Collinge, J. Prion diseases of humans and animals: their causes and molecular basis. *Annu. Rev. Neurosci.* **24,** 519–550 (2001).
25. Chernoff, Y. O. *et al.* Evolutionary conservation of prion-forming abilities of the yeast Sup35 protein. *Mol. Microbiol.* **35,** 865–876 (2000).
26. Kushnirov, V. V., Kochneva-Pervukhova, N. V., Chechenova, M. B., Frolova, N. S. & Ter-Avanesyan, M. D. Prion properties of the Sup35 protein of yeast *Pichia methanolica*. *EMBO J.* **19,** 324–331 (2000).
27. Nakayashiki, T., Ebihara, K., Bannai, H. & Nakamura, Y. Yeast [PSI+] "prions" that are crosstransmissible and susceptible beyond a species barrier through a quasi-prion state. *Mol. Cell* **7,** 1121–1130 (2001).
28. Resende, C. *et al.* The *Candida albicans* Sup35p protein (CaSup35p): function, prion-like behaviour and an associated polyglutamine length polymorphism. *Microbiology* **148,** 1049–1060 (2002).
29. Scott, M. *et al.* Transgenic mice expressing hamster prion protein produce species-specific scrapie infectivity and amyloid plaques. *Cell* **59,** 847–857 (1989).
30. Prusiner, S. B. *et al.* Transgenic studies implicate interactions between homologous PrP isoforms in scrapie prion replication. *Cell* **63,** 673–686 (1990).
31. Collinge, J. *et al.* Unaltered susceptibility to BSE in transgenic mice expressing human prion protein. *Nature* **378,** 779–783 (1995).
32. Supattapone, S. *et al.* Prion protein of 106 residues creates an artificial transmission barrier for prion replication in transgenic mice. *Cell* **96,** 869–878 (1999).
33. Bruce, M. *et al.* Transmission of bovine spongiform encephalopathy and scrapie to mice: strain variation and the species barrier. *Phil. Trans. R. Soc. Lond. B* **343,** 405–411 (1994).
34. Tanaka, M., Chien, P., Yonekura, K. & Weissman, J. S. Mechanism of cross-species prion transmission: An infectious conformation compatible with two highly divergent yeast prion proteins. *Cell* **121,** 49–62 (2005).
35. Hill, A. F. *et al.* The same prion strain causes vCJD and BSE. *Nature* **389,** 448–450 (1997).
36. Chien, P., DePace, A. H., Collins, S. R. & Weissman, J. S. Generation of prion transmission barriers by mutational control of amyloid conformations. *Nature* **424,** 948–951 (2003).
37. Collinge, J., Sidle, K. C., Meads, J., Ironside, J. & Hill, A. F. Molecular analysis of prion strain variation and the aetiology of 'new variant' CJD. *Nature* **383,** 685–690 (1996).
38. Mukhopadhyay, S., Krishnan, R., Lemke, E. A., Lindquist, S. & Deniz, A. A. A natively unfolded yeast prion monomer adopts an ensemble of collapsed and rapidly fluctuating structures. *Proc. Natl Acad. Sci. USA* **104,** 2649–2654 (2007).
39. Krishnan, R. & Lindquist, S. L. Structural insights into a yeast prion illuminate nucleation and strain diversity. *Nature* **435,** 765–772 (2005).
40. Kajava, A. V., Baxa, U., Wickner, R. B. & Steven, A. C. A model for Ure2p prion filaments and other amyloids: the parallel superpleated β-structure. *Proc. Natl Acad. Sci. USA* **101,** 7885–7890 (2004).
41. Shewmaker, F., Wickner, R. B. & Tycko, R. Amyloid of the prion domain of Sup35p has an in-register parallel β-sheet structure. *Proc. Natl Acad. Sci. USA* **103,** 19754–19759 (2006).
42. Ross, E. D., Edskes, H. K., Terry, M. J. & Wickner, R. B. Primary sequence independence for prion formation. *Proc. Natl Acad. Sci. USA* **102,** 12825–12830 (2005).
43. Ross, E. D., Baxa, U. & Wickner, R. B. Scrambled prion domains form prions and amyloid. *Mol. Cell. Biol.* **24,** 7206–7213 (2004).
44. DePace, A. H., Santoso, A., Hillner, P. & Weissman, J. S. A critical role for amino-terminal glutamine/asparagine repeats in the formation and propagation of a yeast prion. *Cell* **93,** 1241–1252 (1998).
45. King, C. Y. Supporting the structural basis of prion strains: induction and identification of [PSI] variants. *J. Mol. Biol.* **307,** 1247–1260 (2001).
46. Serio, T. R. *et al.* Nucleated conformational conversion and the replication of conformational information by a prion determinant. *Science* **289,** 1317–1321 (2000).
47. Glover, J. R. *et al.* Self-seeded fibers formed by Sup35, the protein determinant of [PSI+], a heritable prion-like factor of *S. cerevisiae. Cell* **89,** 811–819 (1997).
48. Heckman, D. S. *et al.* Molecular evidence for the early colonization of land by fungi and plants. *Science* **293,** 1129–1133 (2001).
49. Nelson, R. *et al.* Structure of the cross-β spine of amyloid-like fibrils. *Nature* **435,** 773–778 (2005).
50. Zhao, Z. G., Im, J. S., Lam, K. S. & Lake, D. F. Site-specific modification of a single-chain antibody using a novel glyoxylyl-based labeling reagent. *Bioconjugat. Chem.* **10,** 424–430 (1999).

Supplementary Information is linked to the online version of the paper at www.nature.com/nature.

Acknowledgements We thank J. Weissman for providing the CaNM and Sc/Ca NM chimaera plasmids, M. Schutkowski for assistance in designing and preparing the peptide arrays, N. Watson for performing the transmission electron microscope imaging and members of the Lindquist laboratory for helpful discussions. This research was supported by an American Cancer Society Postdoctoral Fellowship (P.M.T.), and grants from the DuPont-MIT Alliance and the NIH. S.L. is an Investigator of the Howard Hughes Medical Institute.

Author Contributions Experimental work was performed by P. Tessier, and the data analysis and writing were conducted by P. Tessier and S. Lindquist.

Author Information Reprints and permissions information is available at www.nature.com/reprints. The authors declare no competing financial interests. Correspondence and requests for materials should be addressed to S.L. (lindquist_admin@wi.mit.edu).

METHODS

Mutagenesis, protein purification and cysteine labelling. Single cysteine mutations were introduced into NM using QuikChange mutagenesis (Stratagene). All NM proteins were purified as described previously[47] except that the proteins were eluted from a Ni-NTA column using low pH instead of imidazole. The NM cysteine mutants at or near the C terminus (*S. cerevisiae* A230C, *C. albicans* S227C and all chimaeras at the extreme C terminus) were labelled overnight at room temperature with maleimide-functionalized Alexa Fluor 555 or 647 (Invitrogen) using a 5:1 to 10:1 molar ratio of label:NM, and the free label was removed using a Ni-NTA column.

Peptide array synthesis, hybridization and quantification. Peptides were synthesized on modified cellulose membranes using SPOT technology[51] (JPT Peptide Technologies GmbH). The peptides were cleaved off the membranes, freeze-dried and resuspended in buffer (40% DMSO, 5% glycerol, 55% PBS, pH 9) for printing. The peptides were then printed in triplicate onto hydrogel glass slides (Nexterion Slide H, Schott) and immobilized via reactive *N*-hydroxysuccinimide (NHS) ester moieties. (It is recommended to print each peptide 4–6 times per array for improved statistics.) Each peptide spot (250 μm in diameter) was printed with 1.5 nl of peptide solution at a concentration of approximately 2.5 μM using non-contact printing (JPT Peptide Technologies GmbH). Unreacted peptides were removed from the hydrogel slides. Slides were dried and blocked with 3% BSA in PBST for 1 h. The NM proteins were denatured in 6 M guanidine hydrochloride at 100 °C for approximately 20 min, and then diluted 125-fold in PBST containing 3% BSA to a final concentration of 1–5 μM NM and a label-per-protein molar ratio of 5–75%. Each peptide array was incubated individually with 2–3 ml of diluted NM in an Altas hybridization chamber (BD Biosciences) for the indicated times without mixing. The peptide arrays were then washed 5 times with 50 ml of 2% SDS for 30 min, 5 times with 50 ml of water, 3 times with 50 ml of methanol and then spun dry. The methanol washes were not essential but helped prevent uneven drying of the slides. The arrays were then imaged using a Genepix 4000A scanner and the median fluorescence values of two or three replicates for the peptide spots were quantified using Genepix Pro 6.0 software (Molecular Devices). The Genepix composite pixel intensity (CPI) threshold was varied between different experiments to illustrate differences in protein interaction specificity.

51. Frank, R. The SPOT-synthesis technique. Synthetic peptide arrays on membrane supports–principles and applications. *J. Immunol. Methods* **267**, 13–26 (2002).